PHYSICAL REVIEW B VOLUME 2, NUMBER 1 1 JULY 1970

Specific Heat of CoO near T_N: Anisotropy Effects*

M. B. Salamon
Department of Physics and Materials Research Laboratory, University of Illinois, Urbana, Illinois 61801
(Received 29 December 1969)

The specific heat of CoO single crystals has been measured near the Néel temperature, using steady-state ac calorimetry. The critical exponents are found to be $\alpha' = 0.05 \pm 0.02$ and $\alpha = 0.12 \pm 0.01$, which are very close to the predictions of the three-dimensional Ising model. Further, the actual values of the data (relative to pure copper) are fitted very closely above T_N by the analytic form of the Ising specific heat. Recent theories have predicted Ising-like behavior near T_N for slightly anisotropic exchange Hamiltonians. From a calculation of the effective spin Hamiltonian, it is found that a local pseudodipolar term is induced by magnetostriction. Use of a pair-cluster approximation shows that this local anisotropy is proportional to the short-range order parameter and persists above T_N. At T_N, the ratio $J_\parallel/J_\perp$ is found to be about 1.02. This leads to the prediction of Ising-like behavior for $|T/T_N - 1| \lesssim 10^{-2}$, which is borne out by the data.

I. INTRODUCTION

In real magnetic materials, anisotropy often plays a role nearly as important as the exchange interaction. Yet, until recently,[1-3] anisotropy has been ignored in studies of the critical behavior.

In cubic materials, anisotropy effects are most important in crystals containing rare-earth ions or iron-group ions with unquenched angular momentum. A classic example is CoO, which undergoes a tetragonal distortion below the Néel temperature. The residual angular momentum of the Co ion is locked along the tetragonal axis at low temperature, and, in turn, through the spin-orbit coupling, aligns the spin antiparallel to the angular momentum. As a result, the spin of the ion has only one quantization axis (for the ground-state doublet) and therefore approximates an Ising antiferromagnet.

Jasnow and Wortis[1] have hypothesized that the behavior of a magnetic system near its critical point has a one-to-one correspondence to the symmetry of the ground state. If so, CoO should behave like an Ising antiferromagnet near T_N. Riedel and Wegner[2] have extended the argument to show that for any nonzero anisotropy, the critical behavior must become anisotropic near enough to T_N. Below some temperature, the growth of transverse fluctuations is limited by the uniaxial anisotropy and the critical behavior becomes that appropriate to the lower symmetry.

We report here the results of specific-heat measurements on single crystals of CoO made using steady-state ac calorimetry. The critical exponents α and α' are found to be very close to the predictions of the three-dimensional Ising model,[3] with $\alpha' \cong 0.05$ and $\alpha \cong 0.12$. It is shown that the actual heat capacity of the sample can be estimated directly from the ac data. Using the estimated values, we find that the specific-heat data for $T > T_N$ are fitted quite closely by the theoretical Ising specific heat. Below T_N, the amplitude of the observed singularity is much smaller than predicted, although the critical exponent is the same.

Using crystal field theory,[4] we calculate the spin Hamiltonian for CoO near T_N and use it to estimate the temperature dependence of the local anisotropy in the Oguchi[5] approximation. The values of the anistropic terms in the spin Hamiltonian are estimated and found to predict Ising-model behavior in the Riedel-Wegner theory.

The size of the lattice contribution to the specific heat is discussed briefly and found to be in rough agreement with a corresponding states analysis of the specific heat of VO.[6]

II. EXPERIMENTAL RESULTS

Samples of CoO were cleaved from a large single crystal used previously for ultrasonic studies.[7] The slices were selected for thinness (the thinnest being about 0.1 mm) and annealed for 1 week at 1000 °C. A check of the density after annealing showed that the samples were of the dense phase of CoO.[8] A 1-mil chromel-alumel thermocouple was cemented to the center of each sample, and the sample mounted parallel to a copper block as shown in Fig. 1. Copper blocks in good thermal contact with the main heat sink were used as cold junctions for the sample thermocouple. The entire assembly was placed in a He atmosphere. Pulses of light from a quartz-iodide lamp provided periodic heating of the sample at frequency ω.

To determine the temperature oscillations $u(x)$ at $x = d$, we solve the diffusion equations

$$\frac{\partial u_{g,s}}{\partial t} = D_{g,s} \frac{\partial^2 u_{g,s}}{\partial x^2} \quad , \tag{2.1}$$

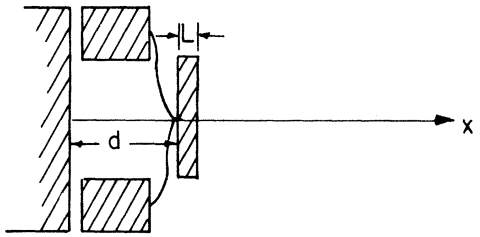

FIG. 1. Sketch of the experimental arrangement. The sample, of thickness L, is placed a distance d from a copper heat sink.

where $D_{g,s}=(\kappa_{g,s}/\rho_{g,s}c_{g,s})$ and $\kappa_{g,s}$, $\rho_{g,s}$, and $c_{g,s}$ are the thermal conductivity, density, and specific heat per gram of the gas and sample, respectively. The diffusion of heat pulses through the sample is governed by the propagation constants $k_{g,s}=(1+i)\times(\omega/2D_{g,s})^{1/2}$. The finite thermal conductivity of the sample causes it to act as a low-pass filter for heat pulses. The condition that the sample be in internal thermal equilibrium is equivalent to requiring that the attenuation and phase shift of the pulses be small, that is, that $|k_s|L \ll 1$.

Solutions of (2.1) have the form[9] $u_s(x)=a\cosh k_s\times(x-d)+b\sinh k_s(x-d)$ and $u_g(x)=c\sinh k_g x$. Since $|k_s|L$ is small, it is possible to expand $u_s(x)$ and $u_s'(x)$ as

$$u_s(x)=a+bk_s(x-d)\quad,$$
$$u_s'(x)=bk_s+ak_s^2(x-d)\quad. \tag{2.2}$$

Matching the temperatures and heat flows at the two surfaces of the sample we find that

$$aLk_s+b=-P/\kappa_s k_s A$$

and $$b/a=(\kappa_g k_g/\kappa_s k_s)\coth k_g d\quad,$$

where P/A is the net heat flux entering the sample per second at $x=d+L$. Thus, the temperature at the surface $x=d$ is given by

$$u_s(d)=\frac{-P}{k_s^2\kappa_s LA}\left(1+\frac{\kappa_g k_g\coth k_g d}{\kappa_s k_s^2 L}\right)^{-1}\quad. \tag{2.3}$$

The first factor in (2.3) is equal to $iP/\omega C_s$, where C_s is the heat capacity of the sample. The denominator contains the term $k_g d\coth(k_g d)/\omega\tau$, where $\tau=C_s d/\kappa_g A$. In order to measure only the heat capacity of the sample, we require that this term be small, that is, that $\omega\tau\gg 1$ ($x\coth x\lesssim 1$). Under the conditions of this experiment, $\omega\tau\cong 500$ and $|k_g|d\cong 1$. Unfortunately, even for the thinnest CoO samples $|k_s|L$ is nearly unity. This can lead to a small correction factor in (2.3) but only to a negligible (<1 mK) gradient across the sample. A more detailed analysis has been given by Schwartz[9] with very similar results.

The temperature oscillations of the sample are processed by an HR-8 lock-in amplifier which records the rms amplitude of the fundamental frequency f of the input signal. Since the power input to the sample is a square wave of amplitude P, the actual temperature rise is

$$u_{ac}=0.707P/\pi^2 fC_s\quad. \tag{2.4}$$

In addition, there is a dc component

$$u_{dc}=Pd/2\kappa_g A\quad. \tag{2.5}$$

By measuring both components, we can eliminate the power P from (2.4), which then becomes

$$u_{ac}=(1.414\kappa_g u_{dc}/\pi^2 fld\,\rho_s^{-1})c_s^{-1}. \tag{2.6}$$

Using standard values for κ_g in (2.6), we have obtained the heat capacity of samples of pure copper which are within 10% of the absolute values found in the literature and which follow the temperature dependence to within 1%. The principal error in (2.6) appears to arise from the assumption of simple one-dimensional heat flow in the gas. For the CoO data, the value of κ_g/d which gives the best fit for copper samples was used. This choice leads to a C_p, which is as much as 20% smaller than the results of Assayag and Bizette.[10] In view of this and the approximations leading to (2.6), we must consider the absolute magnitude of our results to be only approximate.

Values of u_{ac} and the temperature of the sample are recorded continuously as the temperature of the heat sink is slowly varied (about 400 mK/h). No hysteresis was observed and the data are consistent from run to run and from sample to sample. The temperature rise of the sample is about 4 mK/pulse, which limits our resolution. The raw data are converted to temperature oscillations using the slope of the emf-versus-temperature curve for the chromel-alumel thermocouple, and then fit to the usual power-law form of the heat capacity[3] by a least-squares procedure. This program sorts the data according to the current estimate of the Néel temperature and fits the entire curve at once.

The result of a fit of 100 points within $|\epsilon|=5\times10^{-2}$ of the Néel temperature for a single run gives

$$C_H^-/R=(0.09/\alpha')(|\epsilon|^{-\alpha'}-1)+0.76 \tag{2.7}$$

and $$C_H^+/R=1.12(\epsilon^{-\alpha}-1)\quad, \tag{2.8}$$

where $0.03\lesssim\alpha'\lesssim 0.06$ and $\alpha=0.12\pm0.01$. The lattice background amounts to $C_L/R=3.92+4.85\epsilon$. With these parameters, the rms deviation of the data from calculated values is 0.8%. The errors in the critical exponents give the range of values for which the increase in χ^2 is less than 1%. These errors are approximately the same as the most probable errors, which occur in the least-squares

error matrix.[11] The data can also be fitted to a logarithmic specific-heat curve below T_N of the form $C_H^-/R = -0.1 \ln|\epsilon| + 0.80$, but with an rms deviation of about 1.2%. In either case, the exponents are surprisingly like the predictions of the three-dimensional Ising model[3] and, for the high-temperature data, the strength of the singularity is also very close to the Ising model.[12] In all of the above, we have taken $\epsilon = (T/288.46\ \mathrm{K}) - 1$.

In Fig. 2, we have plotted the high-temperature data for several runs relative to the sloping lattice background determined by the least-squares fit. On the same graph the theoretical predictions of the Ising model[12] (solid curve) and the Heisenberg model[13] (dashed curve), for which α and $\alpha' \lesssim 0$, are drawn relative to the same base line. The fit of the Ising curve to the data is extremely good, even better than the power-law curve used in the least-squares analysis. We stress that although the scale of this figure is determined from (2.6) using values obtained from the specific heat of pure copper, it is in disagreement with earlier work[10] and the excellent fit may be fortuitous. A scale error will not, of course, affect the values of the critical exponents.

The situation below T_N is much less clear. The critical index α' is close to the Ising value[3] as can be seen in Fig. 3. There, the solid curve is the result of setting $\alpha' = 0.05$ in (2.7). However, the theoretical curve[14] (dashed line) is a factor of 3 larger. Gaunt and Domb have suggested[14] that the low-temperature specific-heat curve might be rounded as much as two decades farther from T_N than the high-temperature curve. We may, therefore, be observing only the rounding of an Ising-like specific heat.

Finally, we note that there is little difference

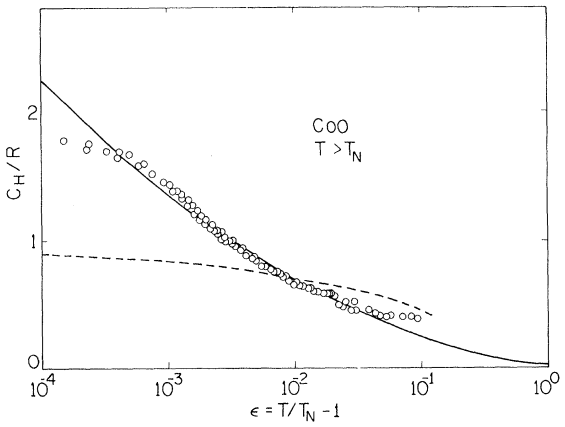

FIG. 2. Specific heat of CoO for $T > T_N$. The solid curve is the three-dimensional Ising specific heat (Ref. 12); the dashed curve, the specific heat of the three-dimensional Heisenberg model (Ref. 13).

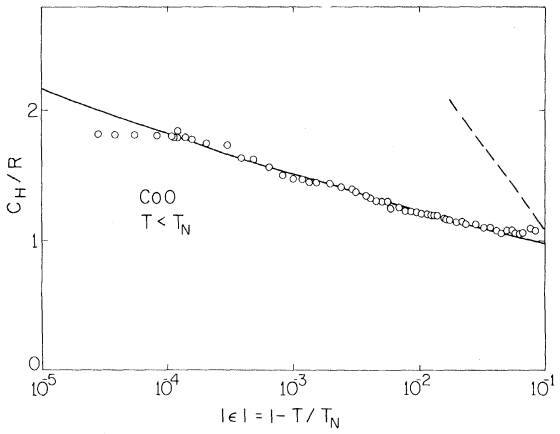

FIG. 3. Specific heat of CoO for $T < T_N$. The solid curve is a power-law fit to the data with $\alpha' = 0.05$. The dashed curve is the predicted specific heat of the three-dimensional Ising model which has $\alpha' = \frac{1}{16}$, but larger amplitude (Ref. 15).

between c_p and c_v per unit volume near the critical point of CoO. We use the usual thermodynamic relation $c_p - c_v = T\beta^2/K_T$ and the Pippard relation[15] $\beta = c_p/T\xi$, where $\xi = (dP/dT)_{T=T_\lambda}$. The isothermal compressibility K_T has a much smaller anomaly (of order $c_p/T\xi^2$), which we ignore. The slope of the λ line is large for CoO with $\xi = 1.7\times10^3$ bar/K.[16] The result, then, is that

$$c_v = c_p(1 - c_p/T\xi^2K_T) \quad . \tag{2.9}$$

At the peak in the c_p curve, the correction factor is at most $\frac{1}{20}$. This may be responsible for the slightly steeper rise in the measured c_p curves very near T_N.

III. SPIN HAMILTONIAN THEORY

In this section, we discuss the origin of an anisotropic exchange interaction between Co ions and its effect on the critical behavior. The Hamiltonian of the crystal field ground state is assumed to contain a strain-induced tetragonal term which leads to the anisotropy in the spin Hamiltonian. The average pair energy calculated from this Hamiltonian is lower than for the isotropic case and it is this reduction in pair energy which drives the magnetostriction. By minimizing the pair energy, we find that local strain is proportional to the short-range order parameter and, therefore, persists above T_N.

In addition to the tetragonal distortion, there is a rhombohedral distortion which is 10^{-2} times smaller. This additional distortion tips the spins away from the tetragonal axis.[17] Because this is a small effect, we shall ignore it in favor of the tetragonal term.

The unusual properties of CoO arise from the

failure of the cubic crystal field to completely quench the orbital angular momentum of the ^4F ionic state.[4] Under the action of the cubic field, the triplet Γ_4 state is split from the excited Γ_5 and Γ_2 states by about 10 000 cm^{-1}. The triplet state can be assigned a fictitious orbital quantum number l, of unit magnitude, whose matrix elements are related to the actual orbital operator $\vec{L}$ by $\vec{l} = -\frac{2}{3}\vec{L}$.[18] Using this fictitious operator, we can write the Hamiltonian for a single ion, which operates only in the ground state Γ_4 manifold, as

$$\mathcal{H}_0 = \lambda' \vec{l}\cdot\vec{S}_0 - \beta e_{zz}(2l_z^2 - 3) + 2\sum_{j=1}^{z} J\vec{S}_j\cdot\vec{S}_0 \quad . \tag{3.1}$$

The effective spin-orbit coupling constant is $\lambda' = -\frac{3}{2}\lambda$, where $\lambda = -180\ cm^{-1}$. We have not included the effect of admixing the Γ_4 part of the excited ^4P level which reduces λ' slightly.[4] The second term takes account of the tetragonal distortion e_{zz} in the z direction. Kanamori[4] has estimated that $\beta = 7000$ cm^{-1} from the observation of a 1% strain at low temperatures. In the exchange term, the sum is only over the z next-nearest neighbors of the ion since, for the magnetic structure of CoO, there are equal numbers of nearest neighbors on each of the magnetic sublattices. The contributions from nearest neighbors therefore tend to cancel.

We can anticipate the result of diagonalizing (3.1) by considering the terms as successive perturbations on the Γ_4 level. With the spin $S = \frac{3}{2}$ included, the ground state has twelve-fold degeneracy. Denoting the representation of the $S = \frac{3}{2}$ rotation operator under the symmetry operations of the cubic point group by $D_{3/2}$, we can decompose the direct product representation as[19]

$$\Gamma_4 \times D_{3/2} = \Gamma_6 + \Gamma_7 + 2\Gamma_8 \quad . \tag{3.2}$$

Since we expect $\vec{j} = \vec{l} + \vec{S}$ to remain a good quantum number, we make the identification shown in Fig. 4. For CoO, $\lambda' > 0$, and the $\Gamma_6(j = \frac{1}{2})$ level lies lowest. Under the action of the tetragonal field, the upper levels are split into doubly degenerate states while the ground state is unaffected, as sketched in Fig. 4. The remaining degeneracy is lifted by the exchange interaction.

The Hamiltonian (3.1) without the exchange term has been diagonalized for general values of βe_{zz} by Abragam and Pryce.[18] For $\beta e_{zz} = 0$, they obtain

$$E(\Gamma_8) - E(\Gamma_6) = 405\ cm^{-1} \quad .$$

The splitting is not large compared with $k_B T_N$, but we will nevertheless consider only the ground state in constructing the spin Hamiltonian.

In the presence of a small strain, the eigenvalue equation can be solved to first order in e_{zz}. The result for the splitting between the lowest Δ_6 levels is

$$E_2(\Delta_6) - E_1(\Delta_6) = 405(1 - 4\Delta/15)\ cm^{-1} \quad , \tag{3.3}$$

where $\Delta = 2\beta e_{zz}/\lambda'$. Starting from the states $|m_l m_s\rangle$ for which $l_z = m_l$ and $S_z = m_s$, we find that the eigenfunctions corresponding to the ground-state Δ_6 doublet are

$$\psi_{\pm 1/2} = a\,|\mp 1, \pm\tfrac{3}{2}\rangle + b\,|0, \pm\tfrac{1}{2}\rangle + c\,|\pm 1, \mp\tfrac{1}{2}\rangle \quad ,$$

where

$$\begin{aligned} a &= (1 + 5\Delta/36)/\sqrt{2} \quad , \\ b &= -(1 - 7\Delta/36)/\sqrt{3} \quad , \\ c &= (1 - \Delta/36)/\sqrt{6} \quad . \end{aligned} \tag{3.4}$$

Near the Néel temperature, the effective exchange field at each ion is small and will simply split the ground-state doublet. Therefore, it is convenient to represent the doublet spin by a fictitious $s = \frac{1}{2}$ operator which is related to the matrix elements of the actual spin operator S by

$$\begin{aligned} S_i^z &= \tfrac{5}{3}(1 + 8\Delta/45)s_i^z \quad , \\ S_i^x &= \tfrac{5}{3}(1 - 4\Delta/45)s_i^x \quad , \\ S_i^y &= \tfrac{5}{3}(1 - 4\Delta/45)s_i^y \quad , \end{aligned} \tag{3.5}$$

for the ith ion. In terms of the fictitious spin, the exchange term in (3.1) can be written as

$$\mathcal{H}_0^{ex} = 2J_{eff}\sum_{j=1}^{z}[(1-\delta)\vec{s}_j\cdot\vec{s}_0 + 3\delta s_j^z s_0^z] \quad , \tag{3.6}$$

where $\delta = (8\Delta/45)$, $J_{eff} = 25J/9$, and J is the next-nearest-neighbor exchange energy. Kanamori[4] has estimated J from the transition temperature, from which we find that $J_{eff} \cong 42\ cm^{-1}$ and $\delta \cong 9.2 e_{zz}$. The anisotropic part of (3.6) has the form of a pseudo-dipolar interaction, as it must for spin-$\frac{1}{2}$ ions.

To determine the temperature dependence of δ above T_N, we employ a simple pair model[5] in which each term in (3.6), denoted by $\mathcal{H}_p$, is considered separately. The eigenvalues of $\mathcal{H}_p$ are

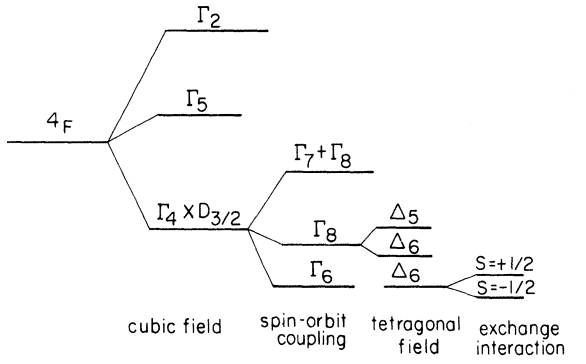

FIG. 4. Energy levels of the Co^{++} ion in CoO, perturbed by successive terms in the Hamiltonian. At low temperatures, the last three terms are nearly equal and must be treated simultaneously. The degeneracy of the Γ_7 and Γ_8 levels results from ignoring Γ_5 and Γ_2 throughout.

$$E_p = J_{\text{eff}}[\tfrac{3}{2} + S'(S'+1)(1-\delta) + 3\delta m'^2], \qquad (3.7)$$

where $S'(S'+1)$ and m' are the eigenvalues of $\vec{S}'^2 = (\vec{s}_j + \vec{s}_0)^2$ and $S'_z = s_j^z + s_0^z$, respectively. Clearly, the ground state is the antiferromagnetic singlet for which $S' = m' = 0$. The anisotropic term in (3.6) splits the $S' = 1$ level thereby lowering the symmetry of the pair. For $T > T_N$, we can calculate the pair energy by taking

$$U_p \cong \frac{3J_{\text{eff}}\,\text{Tr}[\exp(-\mathcal{H}_p/k_BT)s_j^z s_0^z]}{\text{Tr}\exp(-\mathcal{H}_p/k_BT)}.$$

A straightforward calculation gives

$$U_p \cong \frac{3J_{\text{eff}}[-1+e^{-2j}(2e^{-j\delta}-e^{2j\delta})]}{2+2e^{-2j}(2e^{-j\delta}+e^{2j\delta})}\ , \qquad (3.8)$$

where $j = J_{\text{eff}}/k_BT$. Expanding (3.8) for small δ, we find that

$$U_p \cong (\tfrac{1}{2}J_{\text{eff}}\tau_0)(1+2\delta)\ , \qquad (3.9)$$

where $\tau_0 = (-3+3e^{-2j})/(1+3e^{-2j})$ is the pair correlation function in the Oguchi model.[5] Since τ_0 is intrinsically negative, the pair energy is lowered by the strain.

The reduction in pair energy in (3.9) drives the spontaneous magnetostriction of CoO. The cost in elastic energy per pair is $U_e \cong (\Omega_p c_{11}/2)e_{zz}^2$, where Ω_p is the volume per pair. Minimizing the total energy, we find that

$$e_{zz} \cong [-U_m(T)/c_{11}](16\beta/45\lambda')\ , \qquad (3.10)$$

where $U_m(T)$ is the total magnetic energy per unit volume.

Implicit in the derivation of (3.10) is the assumption that the lattice strain can follow the direction of the local magnetization. This is true only if the characteristic time for changes in the local magnetization is long compared with the response time of the lattice, that is, so long as $\xi^2/\Lambda \gg \xi/v_s$, where ξ is the coherence length, Λ is the spin diffusivity, and v_s is the speed of sound. For reasonable values of these quantities, this condition is satisfied throughout the critical region.

We have demonstrated in (3.10) that local anisotropy persists above T_N. The exchange Hamiltonian (3.6) has, therefore, a finite δ which decreases slowly above T_N. Jasnow and Wortis[1] have calculated the critical exponents for a Hamiltonian similar to (3.6) (but not of the pseudodipolar form) and concluded that for any $\delta \neq 0$, the behavior is like the three-dimensional Ising model at T_N, changing abruptly to Heisenberg behavior when $\delta = 0$. Away from the critical temperature, the energy in fluctuations exceeds the anisotropy energy and the behavior becomes isotropic.

This problem has been considered recently by Riedel and Wegner.[2] In their model, the anisotropy parameter δ is scaled as an external field according to $\delta \sim L^{\phi}$, where L is the scaling length, and ϕ is unknown. Riedel and Wegner argue that $\phi \approx \gamma$, the exponent for the static susceptibility. So long as $\epsilon, \delta \ll 1$, the scaling laws for the isotropic case will hold and the singular part of the free energy will scale as

$$F^{\text{sing}}(\epsilon, \delta) = L^{\alpha_i - 2}F^{\text{sing}}(L\epsilon, L^{\phi}\delta)\ , \qquad (3.11)$$

where i refers to the isotropic value of the exponent. This implies that

$$F^{\text{sing}}(\epsilon, \delta) = \epsilon^{2-\alpha_i} w(\delta/\epsilon^{\phi}) \qquad (3.12)$$

and that $w(x)$ becomes constant as $x \to 0$. Similarly, close to T_N the anisotropic scaling laws will hold if $\epsilon^{\phi} \ll \delta$. If so, we will have

$$F^{\text{sing}}(\epsilon, \delta) = L^{\alpha_a - 2}F^{\text{sing}}(L\epsilon, L^{\phi}\delta) \qquad (3.13)$$

and the subscript refers to the anisotropic value of the exponent. In the event that $\epsilon^{\phi} \ll \delta \ll 1$, both forms of the scaling laws are valid and a comparison of (3.12) and (3.13) leads to the conclusion that

$$w(\delta/\epsilon^{\phi}) = (\delta/\epsilon^{\phi})^{(\alpha_i - \alpha_a)/\phi} \qquad (3.14)$$

for δ/ϵ^{ϕ} large. Hence, there is a change from isotropic to anisotropic critical behavior near the temperature $\epsilon \approx \delta^{1/\phi}$. This had been noted earlier by Kawasaki.[20] The argument, stated simply, is that the anisotropy adds a term proportional to the square of the transverse magnetization to the magnetic free energy. The effective transverse susceptibility then becomes $\chi_{\perp}^{-1} = \chi_{\parallel}^{-1} + K$, where K is the anisotropy constant. The transverse susceptibility and, therefore, the transverse fluctuations, cease growing when $\chi_{\parallel}^{-1} \approx K$, which is the same as the crossover deduced from (3.14)

In Fig. 5, we have sketched $\delta(\epsilon)$ as calculated from (3.10), using the area under the specific-heat curve to estimate $U_m(T)$. The dashed curve sepa-

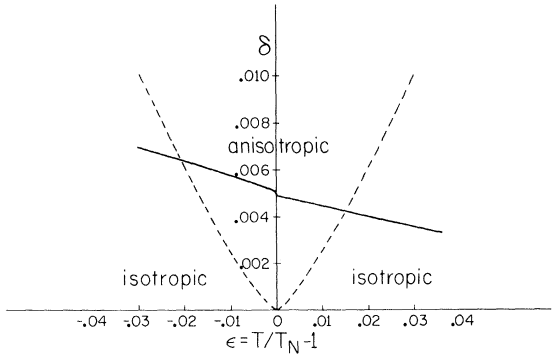

FIG. 5. Strain-induced local anisotropy parameter. The temperature dependence is calculated from the area under the specific-heat curve. The broken lines separate the isotropic and anisotropic regions predicted by the Riedel-Wegner theory (Ref. 2).

rates the anisotropic and isotropic regions under the assumption $\phi = \frac{4}{3}$. The crossover to isotropic behavior occurs for $\epsilon \approx 2\times10^{-2}$ and, indeed, the high-temperature data, Fig. 1, begin to deviate from the Ising specific-heat curve near $\epsilon \approx 3\times10^{-2}$. Although it is unjustified to claim that our data show a change in critical exponent, it seems clear that the Riedel-Wegner model provides an explanation for the observation of Ising-like behavior in CoO.

We can also write (3.6) in the form

$$\mathcal{H}_0^{ex} = 2\sum_{j=1}^{z}\left[J_{\parallel}S_j^z S_0^z + J_{\perp}(S_j^x S_0^x + S_j^y S_0^y)\right] \quad ,$$

where $J_{\parallel} = (1+2\delta)J_{eff}$

and $J_{\perp} = (1-\delta)J_{eff}$.

From Fig. 5, we see that, at T_N, $J_{\parallel}/J_{\perp} \cong 1.02$. Thus, even a 2% anisotropy is predicted to affect the critical behavior over a sizable portion of the critical region. We note that the rhombohedral effects will not be noticeable above $|\epsilon| \cong 10^{-4}$.

IV. LATTICE SPECIFIC HEAT

It was found in Sec. II that a linearly increasing lattice background must be subtracted from the data to obtain a good fit to a power law. The linear term has the same slope as the high-temperature data, at which point ($T = 333$ K) the logarithmic derivative of the measured curve is

$$C_p'/C_p = 2\times10^{-3}\ \mathrm{K}^{-1} \qquad (4.1)$$

independent of the calibration. At this temperature, the chromel-alumel thermocouple is fairly linear and will make only a small contribution to (4.1). We can use (4.1) to estimate the magnitude of C_p from specific-heat curves of a similar nonmagnetic substance by a corresponding states argument.

Let us assume that the specific heat of the reference material C_p^r and that of the sample C_p^s are given by the same function of the reduced temperature $\phi(T/\Theta_{r,s})$. Then the logarithmic derivatives are

$$\begin{aligned}(\Theta_r/C_p^r)C_p^{r\prime}(T_r) &= \phi'(x)/\phi(x) \quad ,\\ (\Theta_s/C_p^s)C_p^{s\prime}(T_s) &= \phi'(x)/\phi(x) \quad ,\end{aligned} \qquad (4.2)$$

where $x = T_r/\Theta_r = T_s/\Theta_s$. Since the right-hand sides of (4.2) are equal, we have

$$C_p^{s\prime}(T_s)/C_p^s(T_s) = T_r C_p^{r\prime}(T_r)/T_s C_p^r(T_r) \quad . \qquad (4.3)$$

Reasonably good data are available for VO which has the same NaCl structure as CoO.[6] Comparing the logarithmic derivative of the VO data with the value (4.1) by using (4.3), we conclude that $\Theta_r/\Theta_s \cong 0.8$. At the temperature used in the comparison $C_p^r = 9.9$ cal/mole K, while our calculated value is $C_p^s = 9.8$ cal/mole K. This gives an independent verification of the calibration of the ac specific-heat data and gives some confidence in the scale used in plotting Figs. 2 and 3.

ACKNOWLEDGMENTS

The author is grateful to A. Ikushima for providing the samples for this study and assisting in some of the measurements. The author has benefitted from discussions with M. Wortis and K. Kawasaki.

---

*Work supported in part by the Advanced Research Projects Agency under Contract No. SD-131.

[1]D. Jasnow and M. Wortis, Phys. Rev. 176, 739 (1968).

[2]E. Riedel and F. Wegner, Z. Physik 225, 195 (1969).

[3]L. P. Kadanoff *et al.*, Rev. Mod. Phys. 39, 395 (1967).

[4]J. Kanamori, Progr. Theoret. Phys. (Kyoto) 17, 177 (1956); 17, 197 (1956).

[5]J. S. Smart, *Effective Field Theories of Magnetism* (W. B. Saunders Co., Philadelphia, 1966), pp. 35-44.

[6]S. S. Todd and K. R. Bonnickson, J. Am. Chem. Soc. 73, 3894 (1951).

[7]A. Ikushima, Phys. Letters 29A, 417 (1969).

[8]H. N. Ok and J. G. Mullen, Phys. Rev. 168, 550 (1968).

[9]P. Schwartz, thesis, University of Illinois, 1969 (unpublished); P. F. Sullivan and G. Seidel, Phys. Rev. 173, 679 (1968).

[10]G. Assayag and H. Bizette, Compt. Rend. 239, 238 (1954).

[11]P. R. Bevington, *Data Deduction and Error Analysis for the Physical Sciences* (McGraw-Hill, New York, 1969), pp. 242-245.

[12]D. L. Hunter, thesis, Kings College, London (unpublished), Chap. 7; M. F. Sykes, J. L. Martin, and D. L. Hunter, Proc. Phys. Soc. (London) 91, 671 (1967).

[13]G. A. Baker, H. E. Gilbert, J. Eve, and G. S. Rushbrooke, Phys. Rev. 164, 800 (1967).

[14]D. S. Gaunt and C. Domb, J. Phys. C 1, 1038 (1968); G. A. Baker and D. S. Gaunt, Phys. Rev. 155, 545 (1967).

[15]A. B. Pippard, *Elements of Classical Thermodynamics* (Cambridge U. P., Cambridge, England, 1957), Chap. 9.

[16]W. B. Holzapfel and H. G. Drickamer, Phys. Rev. 184, 323 (1969).

[17]J. Saito *et al.*, J. Phys. Soc. Japan 21, 850 (1966); S. Moss (private communication).

[18]A. Abragam and M. H. L. Pryce, Proc. Phys. Soc. (London) A206, 173 (1951).

[19]M. Tinkham, *Group Theory and Quantum Mechanics*

(McGraw-Hill, New York, 1964), Chap. 4.
[20]K. Kawasaki, Progr. Theoret. Phys. (Kyoto) 39, 285 (1968).

PHYSICAL REVIEW B VOLUME 2, NUMBER 1 1 JULY 1970

Heisenberg Model and Magnetic Insulators*

J. F. Cooke
Solid State Division, Oak Ridge National Laboratory, Oak Ridge, Tennessee 37830
(Received 24 February 1970)

The magnetization and specific heat are calculated on the basis of a Heisenberg model which is thought to be appropriate for the description of the magnetic properties of four insulating copper salts. The calculation includes first- and second-neighbor interactions and is based on a quasimagnon approximation which goes beyond the Hartree-Fock theory. The low-temperature expansions are exact to order T^4, and the results obtained for the transition temperature are consistent with those obtained from the high-temperature series-expansion theory. Good agreement between theory and experiment is obtained over most of the temperature range $T < T_c$.

INTRODUCTION

The Heisenberg model of magnetism is a phenomenlogical model based on the concept of localized spins interacting by means of an exchange mechanism. The discovery and subsequent study of the four copper salts $Cu(NH_4)Cl_4 \cdot 2H_2O$, $CuK_2Cl_4 \cdot 2H_2O$, $CuRb_2Cl_4 \cdot 2H_2O$, and $Cu(NH_4)_2Br_4 \cdot 2H_2O$ has made it possible to test the ability of the Heisenberg model to predict the magnetic properties of insulators. These copper salts are spin-one-half isotropic ferromagnets with the ferromagnetic ions positioned approximately on a body-centered-cubic (bcc) lattice. The transition temperature T_c of each of these salts is high enough so that measurements of the magnetization and specific heat can be obtained above and below T_c, but low enough so that phonon effects can be neglected. The relatively low T_c would make neutron-scattering experiments rather difficult but not impossible to do.

Measurements of the magnetization and specific heat have been obtained by Miedema *et al.*[1,2] They indicated that their low-temperature results could be fitted reasonably well to the low-temperature Heisenberg theory with nearest-neighbor interactions. In an attempt to extend the expression for the specific heat to higher temperature they used an expression which was incorrect because of a double counting of the Hartree-Fock magnon-magnon interaction energy.

Wood and Dalton[3] subsequently pointed out the necessity of including second-neighbor interactions because of the bcc magnetic structure. Their work showed that it was possible to obtain much better agreement between the experimental and theoretical predictions of certain critical constants if second-neighbor interactions were included. They did not attempt to incorporate the effects of magnon-magnon interactions in their analysis of the low-temperature behavior of the salts.

The first attempt at incorporating the effects of the magnon-magnon interaction was done by Loly, who used the Hartree-Fock result with first- and second-neighbor interactions.[4] The magnetization and specific heat were found to be double valued and the magnetization remained nonzero at all temperatures. Loly used a value of T_c obtained from high-temperature series expansions to plot his results as a function of T/T_c and found that he could get reasonable agreement with the experiments up to about 80% of the transition temperature. It was also pointed out that there was some slight dependence of the results on the ratio of second-to-first-neighbor exchange.

There are several problems connected with the use of the Hartree-Fock theory. First, it does not reproduce the correct low-temperature contributions to thermodynamic quantities made by the magnon-magnon interaction. Second, it is necessary to go outside the Hartree-Fock theory in order to obtain a value of the transition temperature so that the results can be obtained as functions of T/T_c.

It is the purpose of this paper to go beyond the Hartree-Fock theory and to obtain expressions for the magnetization and the specific heat for arbitrary $T < T_c$ which include the effects of first- and